OVERLAY MICROSTRIP STRONG COUPLERS

D. P. Andrews *BSc PhD MIET CEng*, Vectawave Technology Ltd.

***Abstract*-Strong coupling microstrip couplers are described, using a multi-layer construction. These couplers achieve much stronger coupling than can be achieved by conventional approaches such as parallel coupled lines and Lange couplers. The structure corresponds with stripline couplers that also use overlay multi-layer construction. With a higher proportion of fields within the dielectric, the structure also offers closer even and odd mode wave velocity when compared with parallel coupled lines.**

The analysis is quasi-static and only deals with zero thickness perfect conductors.

I. INTRODUCTION

OBTAINING strong coupling in microstrip circuits is generally acknowledged as more difficult than say stripline topology, where overlaying lines with multi-layer substrates is an established technique. Depending on etching technique, a pair of single coupled lines can achieve up to 10dB or so coupling, whereas the more elaborate Lange coupler technique achieves coupling in the 3dB region. For stronger coupling, as might be required for example in a wideband multi-section coupler, a multi-layer approach is necessary, but such analysis is practically absent from the literature. The analysis here addresses this absence and shows how strong coupling techniques can be applied with the example of low-cost substrate materials, with line dimensions that are readily achievable using conventional etching techniques.

The analysis is restricted to zero thickness perfect conductors. As most of the electric fields appear between the broad sides of the conductors this is not a serious restriction.

II. THE OVERLAY MICROSTRIP COUPLER

The structure that will be analysed is as shown in Fig. 1 [1]. The top substrate thickness h_1 is typically selected from available laminates. The lower substrate h_2 may well be a single thickness, but might also be a combination of two laminates, the upper being extended over the entire microwave circuit and to which h_1 is bonded, and the lower confined just to the strong coupling region. The relative dielectric constant ε_r is assumed constant in all substrates.

Conductor lines are etched on the upper and lower faces of the top substrate only. The lower substrate is furnished only with a ground plane on its lower face. The conductors are parallel, with the same width and spacing. This is a convenience for an analysis which doesn't lend itself to the more liberal definition of different widths and spacing. Diagonally opposite lines are tied together.

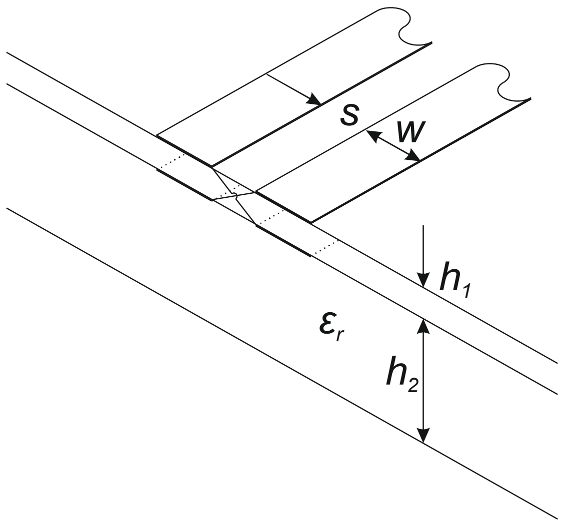

Fig. 1 Diagram of the Overlay Microstrip Coupler

III. LINE CHARGES AND THEIR IMAGES

As we are concerned with a uniform transmission line, we begin our analysis using line charges and investigate the effect of a ground plane and dielectric boundary. The results of this analysis informs us when we develop the line charges into a charge distribution across a strip.

Firstly, let us remind ourselves of the properties of a line charge in free space, as depicted in Fig. 2.

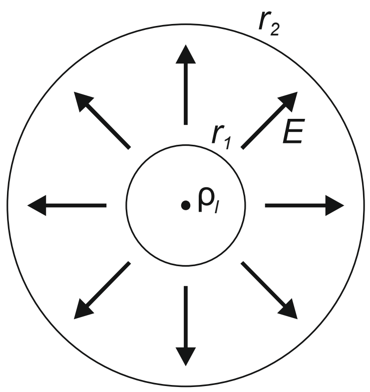

Fig. 2 Line charge in Free Space

The line charge represents a filament of a microstrip line. Electric field is radial, the magnitude of which at a radius r is given by:

$$E = \frac{\rho_l}{2\pi\varepsilon_0 r} \quad (1)$$

The potential between cylinders at radii r_1 and r_2 is given by:

$$V = \frac{\rho_l}{2\pi\varepsilon_0} ln\left(\frac{r_2}{r_1}\right) \quad (2)$$

In both (1) and (2) ε_0 is the permittivity of free space.

Now let us consider the situation where the line charge is parallel to a flat conductor. The radial flux lines are modified especially close to the conductor so they are perpendicular to it, as there can be no electric field across the surface of a conductor. The arrangement can be modelled by an image line charge of equal and opposite value to the original line charge, as depicted in Fig. 3.

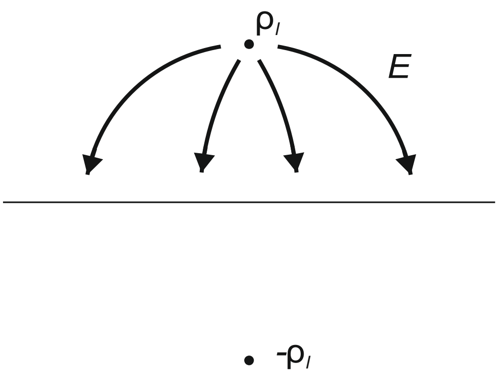

Fig. 3 Electric Field due to a Line Charge over Conductor

The solution to electric field and potential is the superposition of the two line charges. It may be shown that the electric field lines and equi-potentials form circles. Actual charge density is not constant over the conducting surface, but concentrated towards the line directly between the charges.

Note that the image doesn't actually exist, and an excursion to its vicinity will reveal it's absent. It only appears to be present from a point above the conductor plane.

We are interested in the effect of a dielectric interface, as our conductors will be placed either on the surface of a dielectric or below. In this case, we postulate an image above the surface of the dielectric, but of a smaller value than the original line charge.

If a line charge is placed in a dielectric, the effect of the dielectric is to polarise, such that its effective value is reduced by the proportion $1/\varepsilon_r$, where ε_r is the relative dielectric constant. Now let's put this line charge parallel to a dielectric boundary, where the dielectric constant above is ε_0. The line charge polarises the dielectric, such that charge of opposite polarity gathers to it, whilst charge of the same polarity is repelled. The polarisation extends to the dielectric boundary, where it can go no further, resulting in a "bloom" of charge on the surface. We propose this charge appears from within the dielectric as an image the same distance above the boundary as the original charge is below.

From above the dielectric boundary, there is no actual line charge, but the surface charge has the same effect from above as it does below, and creates a modified image coincident with the original line charge.

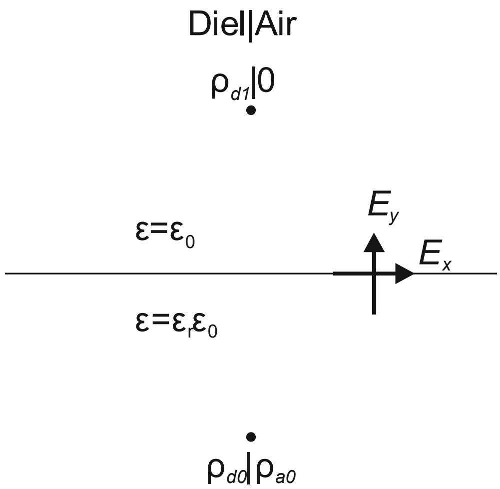

Fig. 4 Line Charge Parallel to Dielectric Boundary

The situation is as shown in Fig. 4, where the apparent line charges vary according to whether they are viewed from within or outside the dielectric. We have (noting the d subscript to refer to the dielectric view and the a subscript the air view):

$$\rho_{d0} = \frac{\rho_l}{\varepsilon_r}, \qquad \rho_{a0} = \rho_{d0} + \rho_{d1}$$

We are interested in determining the value of ρ_{d1}. This may be done by solving the conditions at the boundary. We have in the x-direction:

$$E_{xa} = E_{xd}$$

We know this condition is true, as going from dielectric to air, the image moves from above the boundary to below, so its distance, angle and direction of influence remains the same.

In the y-direction the condition is that the electric field in air is ε_r times the electric field in the dielectric.

$$E_{ya} = \varepsilon_r E_{yd}$$

We thus have:

$$\rho_{d0} + \rho_{d1} = \varepsilon_r(\rho_{d0} - \rho_{d1})$$

Solving for ρ_{d1} and hence for ρ_{a0} we have:

$$\rho_{d1} = \frac{\rho_l}{\varepsilon_r}\left(\frac{\varepsilon_r - 1}{\varepsilon_r + 1}\right) \qquad (3)$$

$$\rho_{a0} = \frac{\rho_l}{\varepsilon_r}\left(\frac{2\varepsilon_r}{\varepsilon_r + 1}\right) \qquad (4)$$

The validity of the assumption regarding an image line charge is borne out by the results holding true at any point on the boundary. The analysis above has made no assumptions about where exactly on the boundary the calculations are made.

Note the apparent intensity of the line charge when viewed from the air is less than the actual line charge and decreases as dielectric constant increases. Although the intensity is fortified by the surface charge, the initial polarization around the line charge is more influential.

We next consider what happens when there is both conductor plane and dielectric boundary. Initially images are created as shown in Fig. 5, where images from the dielectric and air perspectives are tacitly understood from the subscripts.

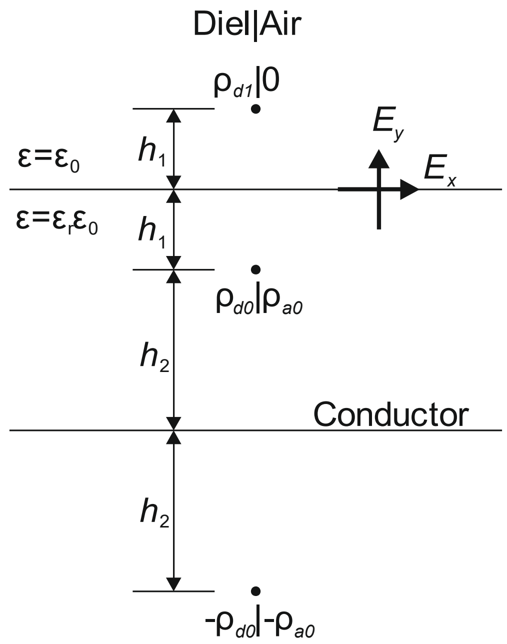

Fig. 5 Initial Images Created by Dielectric Boundary and Conductor Plane

The first two images comprise the perfect image created by the conductor and the partial image of the dielectric boundary. However, conditions at both aren't now met. From the perspective within the dielectric, a further image in the conductor is needed to balance the image of value ρ_{d1}, situated $2h_1$ below the one that's already there. The image below the conductor creates its own polarisation at the dielectric boundary to give a further image $2h_2$ above the one already there.

From the perspective of the air view, the polarisation the additional image below the conductor sets up in the dielectric boundary, appears as an image in the same place. The values of these additional images can be determined by the boundary conditions at the dielectric boundary.

Having added these images, they create the need for further images, propagating from the previous ones at alternate distances of $2h_1$ and $2h_2$. The arrangement begins to look like Fig. 6 (Imagine looking into a mirror with a second one behind your head. Your impression is of an infinite number of images diminishing in intensity as the reflections dissipate).

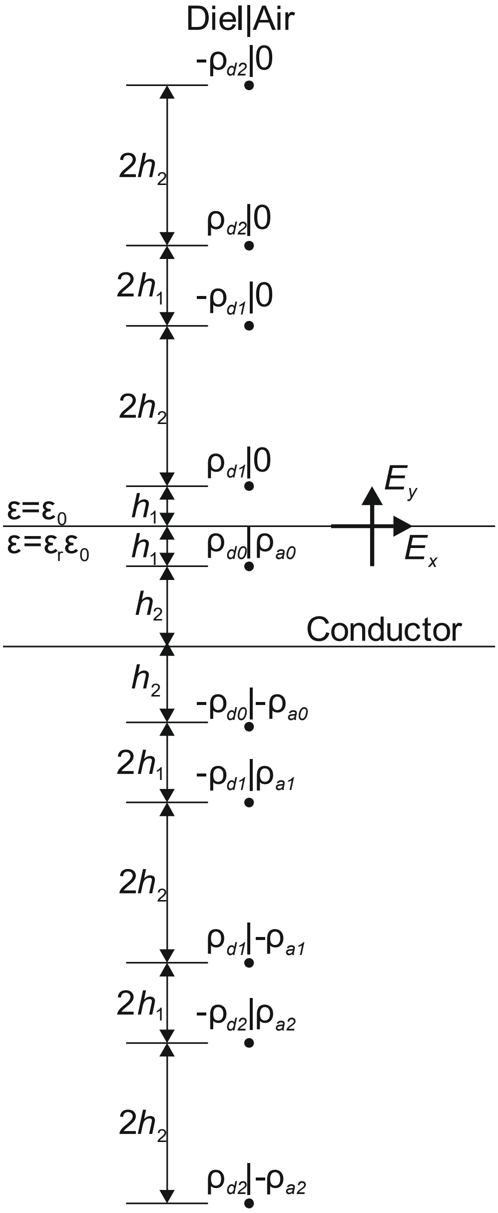

Fig. 6 Images Propagated by Line Charge in Dielectric

Once the initial values have been established, images propagate according to the following formulae:

$$\rho_{d(r+1)} = -\frac{\varepsilon_r-1}{\varepsilon_r+1}\rho_{dr} \tag{5}$$

$$\rho_{a(r+1)} = -\frac{\varepsilon_r-1}{\varepsilon_r+1}\rho_{ar} \tag{6}$$

These images are needed when calculating the potential of a strip to ground or another strip, given a knowledge of the original line charge using (2).

IV. CHARGE DISTRIBUTION IN A STRIP

Having considered a line charge, we now turn to charge distributed over a surface. We look first at a single strip in free space to establish principles before developing them into coupled lines. Its charge distribution can be determined by means of a transformation from the parallel plate arrangement. This is shown in Fig. 7

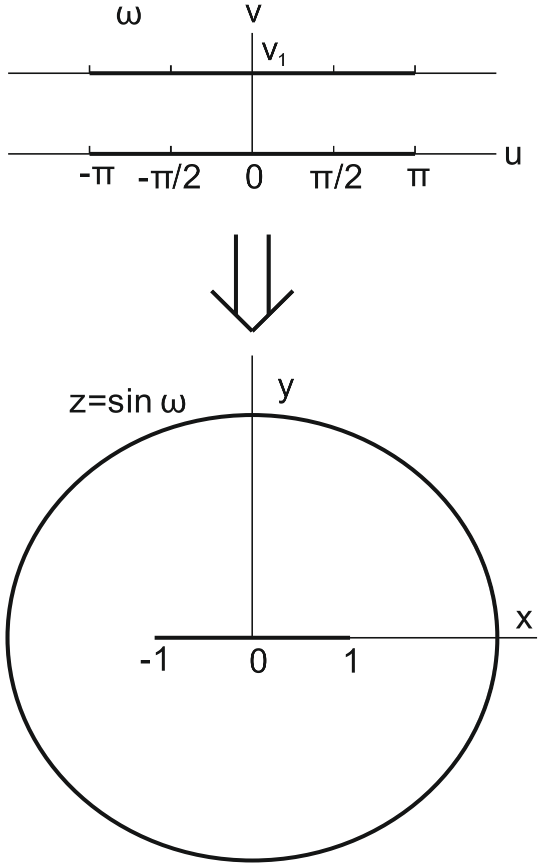

Fig. 7 Transformation from Parallel Plate to Elliptic Coax

For simplicity, we suppose the parallel plate is sectioned into a strip of width 2π. It has one strip at v = 0 and the other at v = v_1. Applying the transformation z = sin ω transforms the lower strip onto the line -1 to 1 and the upper strip onto an ellipse. The lower strip transformation is to a strip that folds at the points -1 and 1 by 180°.

We suppose there to be a uniform surface charge on the plates in the ω-plane. The surface charge density on the plate in the z-plane is equal to twice (because the line is folded) the rate of change of u with respect to x times the surface charge density in the ω-plane, or:

$$\rho_x = 2\frac{du}{dx}\rho_u \tag{7}$$

If the charge density is the ω-plane is $\frac{1}{2\pi}$ for unity total charge, that works out as:

$$\rho_x = \frac{1}{\pi\sqrt{1-x^2}} \tag{8}$$

Note that as v_1 increases, the ellipse the upper strip maps onto rapidly moves away from the strip in the middle which stays the same. There is no change in its surface charge density, which may be taken as the charge density of an isolated strip. Note there are power of -½ singularities to the surface charge density at -1 and 1. For this reason, dealing with the problem using finite element analysis creates uncertainty in where the edge actually is. It would be better to employ analysis that takes the edge singularities into account.

Note too that these singularities are always encountered at the edge of a zero thickness strip. Magnifying the edge drives surrounding conductors further away relatively even if they influence the total charge in the vicinity of the strip edge. The singularities arise because the potential across the strip must be zero at all points, balanced by the distribution of charge. Towards the strip edge, available space for charge to balance between some point and the edge is running out, so it must increase to infinity.

V. CHARGE REDISTRIBUTION IN A PAIR OF STRIPS

The preceding analysis considered what happens with charge distribution in an isolated strip. Suppose we have a second strip in a parallel plate transmission line system, carrying an equal and opposite charge distribution to the first. The second strip influences charge on the first, and by symmetry must have the same but opposite charge distribution. As the second strip is brought closer to the first, the charge distribution given by (8) tends to flatten. At the extreme when the plates are very close, they behave like a parallel plate capacitor, with only the very edge exhibiting the essential power of -½ singularity. The flattening may be represented by expanding the denominator of (8) by the binomial theorem and using it to replace the unity numerator. For the first few terms we have the modified surface charge:

$$\rho_x = \frac{1-\frac{1}{2}x^2-\frac{1}{8}x^4}{\pi\sqrt{1-x^2}}$$

The effect on charge distribution of increasing the order of the numerator can be seen in Fig. 8. The more terms, the better the maximally flat region.

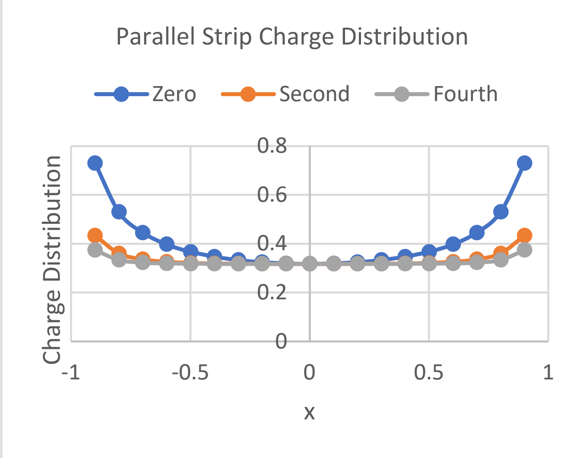

Fig. 8 Charge Distribution with Increasing Approximation Order

In reality, the true coefficients of the numerator terms will be less than as calculated by the binomial theorem and all terms exist. In practice, the closer the plates are together, the more terms are needed to approximate sufficiently. The analysis pivots on optimising the coefficients with the aim of reducing the potential across each plate. If there is no potential the distribution is an authentic representation of a conducting surface. The coefficient of zero order produces no potential along the surface of itself, and we shall call this the *fundamental distribution*. Perturbation of the distributions is created by the second plate, and they respond with a higher order solution.

Analysis of a single plate is applicable to microstrip lines. A second plate corresponds with the image in a ground plane. If further images are introduced because of the dielectric substrate, charge distribution is further modified by these.

VI COPLANAR STRIPS – EVEN MODE

Considering the problem at hand, we are interested in how adjacent strips might be analysed. Let us then consider a pair of coplanar strips. Anticipating analysis in even and odd mode, let us first suppose the two strips are of the same polarity as they are in even mode analysis. Charge isn't symmetrical about the centre of each strip, which tends to accumulate towards the remote edges. A single step transformation isn't obvious, so perform several steps, as follows:

1) $t = sin\omega$
   Transform pair of strips from parallel plane to a strip within an elliptic ground, as for the single strip
2) $p = \frac{1}{2}[(1-k^2)t+1+k^2]$
   Linear transformation of the centred strip

3) $z = \sqrt{p}$
Divides the strip into 2 positions, either side of the vertical axis.

The series of transformations is shown in Fig. 9.

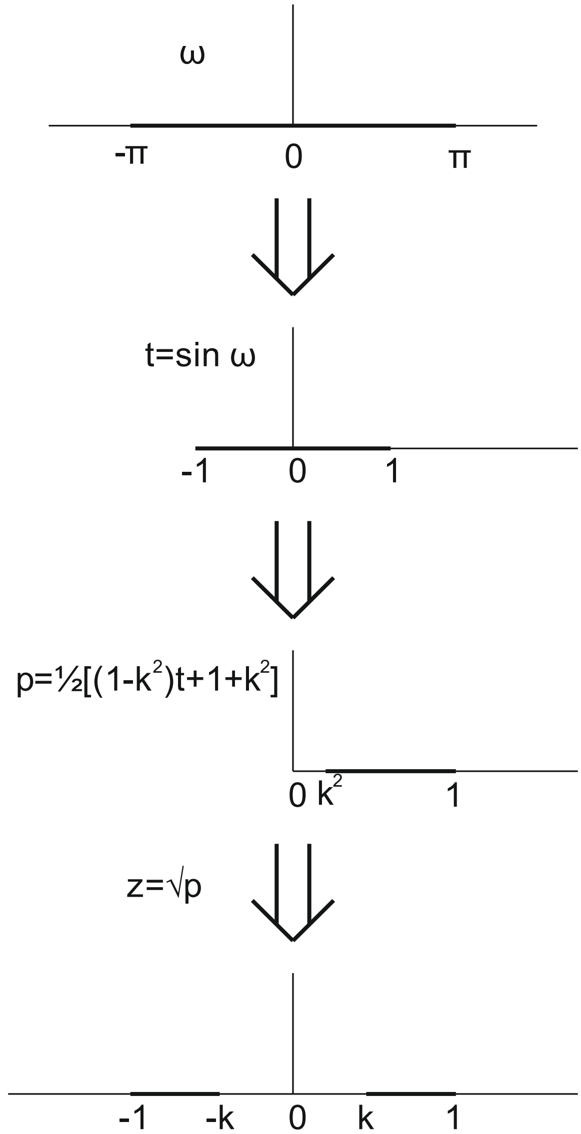

Fig. 9 Transformation to Even Mode Strips

Combining the transformations for the strip in the real axis gives us:

$$x^2 = \tfrac{1}{2}[(1-k^2)sinu+1+k^2] \tag{9}$$

If the original strip has unit charge, applying (8) gives us:

$$\rho_x = \frac{2x}{\pi\sqrt{(1-x^2)(x^2-k^2)}} \tag{10}$$

Let us now develop this even mode fundamental charge density as follows:

$$\frac{x}{\sqrt{(1-x^2)(x^2-k^2)}} = \frac{1}{(1-k)\sqrt{1-\left(\frac{x-k/x}{1-k}\right)^2}}$$

The form under the radical suggests a rendering for an expansion, where we shall use:

$$\rho_{ax} = \frac{x}{\sqrt{(1-x^2)(x^2-k^2)}}(a_0 + a_1X^2 + a_2X^4 \dots)$$

$$X = \frac{x-k/x}{1-k}$$

The problem then becomes one of optimising the a_r coefficients to minimise electric field across a primary strip, given the presence of the secondary strip in the coupled arrangements and both their images. This allows flattening of the charge distribution in the proximity of a strip or image of the opposite polarity. It restricts the minimum charge density point to remain at $\sqrt{k}$. It is convenient to normalise a_0 to unity in the analysis, which becomes the source to generate all the other coefficients.

A similar formula applies to the secondary strip:

$$\rho_{bx} = \frac{x}{\sqrt{(1-x^2)(x^2-k^2)}}(b_1X^2 + b_2X^4 \dots)$$

In this case, the b_0 coefficient is set to zero for convenience of calculation.

Electric field along the x-axis at a point x_0 along the strip is given by:

$$E_x = \frac{gx_0}{\pi\varepsilon_0}\int_k^1 \frac{\rho_x(x_0^2-x^2+y^2)dx}{(x_0^2-x^2)^2+2y^2(x_0^2+x^2)+y^4} \tag{11}$$

Where g is a factor multiplying the effective charge as a result of dielectric loading and the images it creates and y is the vertical distance between the point where electric field is being calculated to the strip with charge distribution contributing to the electric field. The above formula takes into account the corresponding strip at the same y position. Note when determining electric field within a strip using its own charge distribution (where $y = 0$), a singularity occurs at $x = x_0$. This can be avoided by subtracting an auxiliary fundamental charge distribution making it equal to zero at x_0. As a fundamental charge distribution contributes no electric field this won't alter the result. The zero of charge distribution cancels the singularity.

The remaining singularities at the strip edges are eliminated by use of the substitution (9). Nevertheless, the electric field calculation must be evaluated using numerical integration.

Whether the primary strip is taken as one on the surface or one buried (see Fig. 1) is arbitrary, however both options need to be considered in order to solve the even mode capacitance equation. At least as many separate points as unknown coefficients are needed, leading to a matrix of calculations. Oversampling and optimisation are recommended.

Having determined the coefficients, total charge in each strip can be evaluated using the simpler formula:

$$Q_e = \frac{\pi a_0}{2} + \int_k^1 \rho'_{ax} dx$$

Where ρ'_{ax} is the charge distribution without the a_0 term, this being calculable directly via the transformation. The corresponding formula for the secondary strip is also needed.

The next step is to determine the potential between each strip and ground. There are two parts to this calculation. Firstly, the contribution due to the fundamental distribution may be calculated by analytic means, by inverting the transformation to the parallel plate equivalent. The contributions of the remaining coefficients can be determined by integrating the vertical electric field between the ground plane and the plate of interest. The integration has to be performed for all images. Use $x = \sqrt{k}$ as the coordinate for the integration path, where the fundamental distribution is at its minimum and higher order contributions are zero. This procedure avoids the singularity of a finite charge on the integration path.

To determine the analytic part, calculate:

$$v = Im\left[f^{-1}\left(\sqrt{k}, h\right)\right], z = f(\omega)$$

Then:

$$V = \frac{g a_0 v}{4\varepsilon_0}$$

Two values need to be calculated for each primary strip and all its images, as the potential needed is between a target strip and ground. For the higher order coefficients, the potential due to each strip and its images is given by:

$$V = \frac{g}{4\pi\varepsilon_0} \int_k^1 \rho_x log\left[\frac{(y_1+y_2)^4+2(y_1+y_2)^2(x^2+k)+(x^2-k)^2}{(y_1-y_2)^4+2(y_1-y_2)^2(x^2+k)+(x^2-k)^2}\right] dx$$

Where y_1 is the vertical position of the charge distribution and y_2 is the vertical position of the target strip. ρ_x is the charge distribution, omitting the fundamental component for the primary strip and its images.

We need to solve the equation:

$$\begin{bmatrix} Q_a \\ Q_b \end{bmatrix} = \begin{bmatrix} C_{aa} & C_{ab} \\ C_{ba} & C_{bb} \end{bmatrix} \begin{bmatrix} V_a \\ V_b \end{bmatrix} \quad (12)$$

Whilst $C_{ab} = C_{ba}$ according to the principle of reciprocity, there are three unknowns to solve, so it is necessary to calculate values with both the surface and buried strips as primary.

We need to determine even mode capacitance. In addition, inductance per unit length is required in order to determine even mode characteristic impedance. Rather than analysing the line for inductance, it may be calculated according to the knowledge that propagation velocity with no dielectric present is at the speed of light. We then have:

$$c = \frac{1}{\sqrt{L_e C_e}}$$

If we run the capacitance analysis with no dielectric, which is very simple because there are only the two images in the ground plane, we can determine inductance per unit length.

Capacitance per unit length is given by:

$$C_e = C_{aa} + 2C_{ab} + C_{bb}$$

We will have two value of even mode capacitance, one with no dielectric and the other with. Call these C_{ae} and C_{de} respectively. We then have:

$$L_e = \frac{1}{c C_{ae}^2}$$

$$Z_{0e} = \sqrt{\frac{L_e}{C_{de}}}$$

The relative effective even mode dielectric constant is:

$$k_e = \frac{C_{de}}{C_{ae}}$$

$$v_{pe} = \frac{c}{\sqrt{k_e}}$$

VII COPLANAR STRIPS ODD MODE

In this case a single step transformation is applicable. We may use [2]:

$$z = dn(\omega, k')$$

The transformation of the parallel plate section is shown in Fig. 10. The mapping of the points *-K'* and *K'* → *k* and 0 → 1. The lower plate maps onto the right hand and the upper plate similarly but onto the left hand. There is therefore no need to argue about the profile of a return conductor, as that is supplied directly by the transformation.

As the real axis transforms to the real axis, we can determine the differential given by:

$$\frac{du}{dx} = \frac{-1}{\sqrt{(1-x^2)(x^2-k^2)}} = \frac{-1}{\frac{1-k^2}{2}\sqrt{\left[1-\left(\frac{2x^2-1-k^2}{1-k^2}\right)^2\right]}}$$

It doesn't matter for our purposes about the negative sign, as that simply indicates the direction of u as x varies.

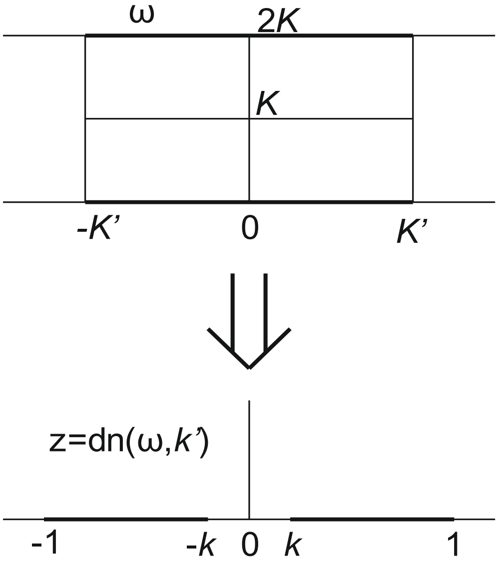

Fig. 10 Transformation to Odd Mode Strips

Following the same procedure as even mode, we may infer a charge distribution given by:

$$\rho_{ax} = \frac{1}{\sqrt{(1-x^2)(x^2-k^2)}}(a_0 + a_1X^2 + a_2X^4 \dots)$$

$$X = \frac{2x^2-1-k^2}{1-k^2}$$

This describes the charge distribution for the primary strip (whether that is one on the surface or the one buried). The a_0 coefficient determines the fundamental distribution – the solution where no other conductors influence a single pair of oppositely charged strips. For the secondary strip, we have similarly:

$$\rho_{bx} = \frac{1}{\sqrt{(1-x^2)(x^2-k^2)}}(b_1X^2 + b_2X^4 \dots)$$

No fundamental distribution is required. Electric field at a point x_0 along the strip being considered is given by:

$$E_x = \frac{g}{\pi\varepsilon_0}\int_k^1 \frac{\rho_x x(x_0^2-x^2-y^2)dx}{(x_0^2-x^2)^2+2y^2(x_0^2+x^2)+y^4}$$

Once again g is the factor attributed to the effective charge in the particular image. The singularity at x_0, when calculating the contribution of charge density within the same strip, can be avoided by subtracting a fundamental distribution with the same charge density at that particular point. The presence of x in the numerator means a trigonometric rather than elliptic substitution may be used to eliminate the singularities at k and 1.

Once the unknown variables (a_r and b_r) have been solved, the total charge in each strip can be determined from:

$$Q_o = K'a_0 + \int_k^1 \rho'_{ax}dx$$

Again, ρ'_{ax} is the charge distribution without the a_0 term and a second calculation is required for the secondary strip using ρ_{bx}.

When determining the potential at each strip, the integration path should be taken where $x = \sqrt{[(1+k^2)/2]}$, so only the fundamental distribution contributes a finite value at the primary strip. This avoids the complication of a singularity in the integration path.

The contribution of the fundamental may be determined using an analytic method. This requires the value of v in the ω plane corresponding to (x,y), which is facilitated by a result of elliptic function analysis. Consider the diagram shown in Fig. 11.

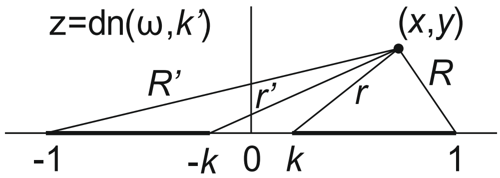

Fig. 11 Construction to Evaluate Elliptic Imaginary Part

From manipulation of elliptic functions, under the transformation $z = dn(\omega,k')$ we have:

$$\frac{R'-R}{r'+r} = \frac{cn\,v}{dn\,v} = sn(K-v)$$

Therefore:

$$v = K - sn^{-1}\left(\frac{R'-R}{r'+r}\right)$$

The potential due to the fundamental distribution is given by:

$$V = \frac{ga_0v}{2\varepsilon_0}$$

The potential due to the remaining coefficients is given by:

$$V = \frac{g}{4\pi\varepsilon_0}\int_k^1 \rho_x log\frac{[(x+x_0)^2+(y_1-y_2)^2][(x-x_0)^2+(y_1+y_2)^2]}{[(x-x_0)^2+(y_1-y_2)^2][(x+x_0)^2+(y_1+y_2)^2]}dx$$

$$x_0 = \sqrt{\frac{1+k^2}{2}}$$

The same logic applies in determining odd mode impedance and relative dielectric constant. With subscripts tacitly understood we determine:

$$C_o = C_{aa} - 2C_{ab} + C_{bb}$$

$$L_o = \frac{1}{cC_{ao}^2}$$

$$Z_{0o} = \sqrt{\frac{L_o}{C_{do}}}$$

$$k_o = \frac{C_{do}}{C_{ao}}$$

$$v_{po} = \frac{c}{\sqrt{k_o}}$$

VIII COMBINING THE MODES

Following well known analysis of even and odd mode couplers, we may determine the characteristic impedance of the structure as:

$$Z_0 = \sqrt{Z_{0o}Z_{0e}}$$

$$Coupling = \frac{Z_{0e}-Z_{0o}}{Z_{0e}+Z_{0o}}$$

With two parameters to vary (*s* and *w*) for a given substrate formula, it is in theory possible to solve for characteristic impedance and coupling. In practice, a minimum coupling is realised for *s* large and maximum coupling subject to fabrication limits. As this is an analysis rather than synthesis procedure, values of *s* and *w* need to be interpolated to find the desired characteristic impedance and the consequential coupling can be calculated, given values from which to produce a graph. Tables of values follow. These have been calculated as overlapping ranges, assuming RO4003 laminate with DK=3.38. The 0.004" material denotes pre-preg to bond two thinner laminates together. A minimum spacing of 0.2mm is assumed, representing sensible etching limits.

w(mm)	s(mm)	Z_{0e}	k_e	k_o	c(dB)
0.506	0.2	103.8	2.85	2.9	-4.1
0.54	0.3	98.5	2.86	2.9	-4.57
0.556	0.4	95	2.87	2.92	-4.94
0.564	0.5	92.3	2.88	2.92	-5.24
0.566	0.6	90.2	2.88	2.93	-5.51
0.564	0.7	88.6	2.89	2.93	-5.74
0.561	0.8	87.1	2.89	2.94	-5.94
0.557	0.9	85.8	2.9	2.94	-6.14
0.552	1	84.7	2.9	2.95	-6.31

Table 1. Coupler Values h1 = 0.032" h2 = 0.032"

w(mm)	s(mm)	Z_{0e}	k_e	k_o	c(dB)
0.759	0.2	124.2	2.76	2.95	-2.84
0.807	0.3	119	2.77	2.97	-3.1
0.833	0.4	115.4	2.77	2.98	-3.3
0.846	0.5	112.7	2.78	2.98	-3.47
0.852	0.6	110.5	2.78	2.99	-3.61
0.853	0.7	108.7	2.79	2.99	-3.73
0.851	0.8	107	2.79	2.99	-3.85
0.847	0.9	105.7	2.8	2.99	-3.96
0.842	1	104.4	2.8	2.99	-4.06

Table 2. Coupler Values h1 = 0.032" h2 = 0.06"

w(mm)	s(mm)	Z_{0e}	k_e	k_o	c(dB)
0.66	0.2	136.6	2.7	3.03	-2.34
0.686	0.3	131.6	2.71	3.04	-2.52
0.696	0.4	128.1	2.72	3.04	-2.67
0.697	0.5	125.4	2.72	3.04	-2.79
0.694	0.6	123.2	2.73	3.04	-2.89
0.689	0.7	121.2	2.73	3.04	-2.98
0.682	0.8	119.6	2.74	3.04	-3.07
0.675	0.9	118	2.74	3.04	-3.15
0.668	1	116.6	2.77	3.04	-3.23

Table 3. Coupler Values h1 = 0.02" h2 = 0.06"

w(mm)	s(mm)	Z_{0e}	k_e	k_o	c(dB)
0.764	0.2	149	2.66	3.07	-1.96
0.794	0.3	144.5	2.67	3.08	-2.1
0.807	0.4	140.7	2.67	3.08	-2.21
0.81	0.5	138	2.68	3.08	-2.3
0.809	0.6	135.8	2.68	3.08	-2.37
0.804	0.7	133.8	2.69	3.08	-2.44
0.798	0.8	132	2.69	3.07	-2.51
0.791	0.9	130.5	2.7	3.07	-2.57
0.784	1	129	2.7	3.07	-2.63

Table 4. Coupler Values h1 = 0.02" h2 = 0.06" +0.016" + 0.004"

w(mm)	s(mm)	Z_{0e}	k_e	k_o	c(dB)
0.711	0.2	159	2.63	3.11	-1.72
0.732	0.3	154.2	2.64	3.12	-1.83
0.74	0.4	150.7	2.64	3.12	-1.92
0.739	0.5	148	2.65	3.11	-1.99
0.735	0.6	145.6	2.65	3.11	-2.06
0.729	0.7	143.6	2.66	3.1	-2.12
0.722	0.8	141.7	2.66	3.1	-2.17
0.714	0.9	140	2.67	3.1	-2.23
0.707	1	138.5	2.67	3.09	-2.28

Table 5. Coupler Values h1 = 0.016" h2 = 0.06" +0.02" + 0.004"

w(mm)	s(mm)	Z_{0e}	k_e	k_o	c(dB)
0.655	0.2	176.7	2.58	3.17	-1.39
0.668	0.3	172	2.59	3.17	-1.47
0.67	0.4	168.4	2.59	3.17	-1.54
0.667	0.5	165.5	2.6	3.16	-1.59
0.661	0.6	163	2.6	3.15	-1.64
0.654	0.7	160.8	2.61	3.14	-1.68
0.646	0.8	158.8	2.61	3.14	-1.73
0.639	0.9	156.9	2.62	3.13	-1.77
0.631	1	155.3	2.62	3.13	-1.81

Table 6. Coupler Values h1 = 0.012” h2 =0.06” +0.032” + 0.004”

Practical values in the region where Lange couplers are most useful can be found in Table 3. Three section 90° couplers require Z_{0e} of at least 150Ω, so Tables 5 and 6 need to be consulted.

IX PRACTICAL DESIGN

In order to test the principles, a coupler was constructed using RO4003 laminate, with h_1 = 0.3mm and h_2 = 2.3mm, s = 0.3mm and w = 0.6mm. Coupling length was 24mm. A photograph of the assembly is shown in Fig. 12.

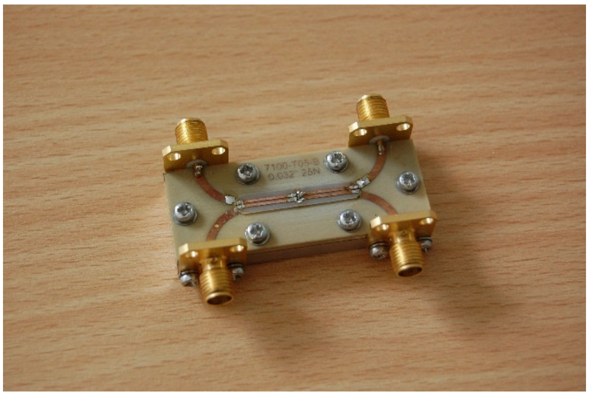

Fig. 12 Photograph of Practical Coupler

The majority of the construction is on a 0.8mm (0.032”) substrate, with an additional booster of 1.5mm (0.06”) in just the coupling area. The lines are printed either side of a 0.3mm (0.012”) substrate bonded to the substrate below.

Running a utility program based on the analysis, the following parameters were predicted:

Z_{0e} = 173.2Ω

Z_{0o} = 15.55Ω

Z_0 = 51.9Ω

k_e = 2.59

k_o = 3.15

The predicted even mode quarter wave frequency is 1.94GHz and odd mode 1.76GHz, yielding an average 1.85GHz. At 1.85GHz a lossless simulation yields -1.58dB coupling, -5.18dB through, 28.6dB input return loss and 30.8dB isolation.

Taking a measurement of the coupler gave the result as shown in Fig. 13.

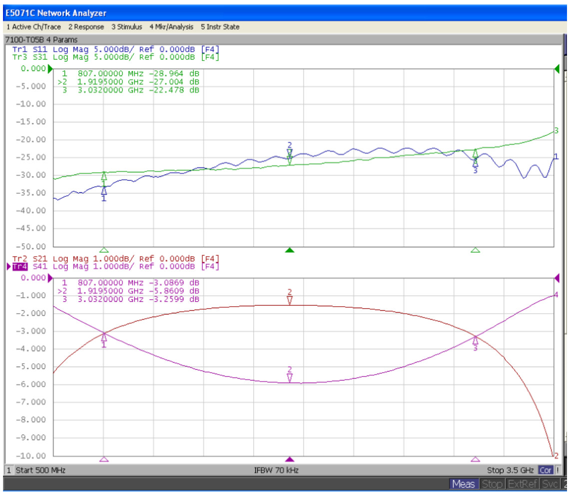

Fig. 13 Measured Performance of a Practical Coupler

Centre frequency is placed at the average of the equal division points. Match and isolation are considered good for this type of construction, regardless of simulation. Coupling of -1.67dB and through loss of -5.84dB correspond with approximately 0.24dB resistive loss, so this value might be added to the coupling figure for a more representative value.

X CONCLUSIONS

An analysis technique for overlay microstrip coupler has been presented. The technique requires the solution of only very few unknowns, these being the coefficients of expansions of charge distribution expressions. The technique avoids inaccuracies associated with finite element analysis at strip edges. The use of microstrip is convenient for integration into microwave circuits and avoids the need to insert stripline components.

XI FURTHER WORK

The restriction of zero thickness lines is not significant for this type of coupler, as much of the coupling takes place between the surfaces of the strips rather than the edge.

A more significant development would be to determine a synthesis program that would generate transmission line parameters for a given characteristic impedance and coupling factor.

REFERENCES

[1] Djordjević, A. R., Napijalo, V. M., Olćan, D. I., and Zajić, A. G., “Wideband multilayer directional coupler with tight coupling and high directivity,” *Microwave and Optical Technology Letters*, vol. 54, no. 10, pp. 2261-2267, 2012.

[2] Bowman, F., *Introduction to Elliptic Functions*, London, England: English Universities Press, 1953.